Metallurgical and Materials Engineering
Association of Metallurgical Engineers of Serbia AMES

Scientific paper
UDC: 66.017/.018
544.2

CONVECTIVE HEAT TRANSFER CHARACTERISTICS OF LOW REYNOLDS NUMBER NANOFLUID FLOW AROUND A CIRCULAR CYLINDER

Yacine Khelili[1], Abderrazak Allali[1], Rafik Bouakkaz[2]*

[1]Department of Mechanical Engineering, University Saad Dahlab, Blida 1, Algeria
[2]Department of Mechanical Engineering, University Constantine 1, Constantine, Algeria.

Received 02.12.2016
Accepted 31.03.2017

Abstract

Numerical investigation of heat transfer phenomena of low Reynolds number nano-fluid flow over an isothermal cylinder is presented in this paper. Steady state governing equations (continuity, N–S and energy equations) have been solved using finite volume method. Stationary heat transfer, and flow characteristics over the cylinder have been studied for water based copper nanofluid with different solid fraction values. The effect of volume fraction of nano-particles on the fluid flow and heat transfer were investigated numerically. It was found that at a given Nusselt number, drag coefficient, re-circulation length, and pressure coefficient increase by increasing the volume fraction of nano-particles.

Keywords: *Nano-fluid steady flow; finite volume; circular cylinder; Reynolds number; volume fraction.*

Introduction

Convective heat transfer can be enhanced by using various methods and techniques, such as increasing the effective heat transfer surface or the heat transfer coefficient. Convection may be used in the local cooling, which is one of the most important technical problems facing many industrial applications. Some of the important applications of convective cooling are microelectronics, transportation, nuclear power plants, cooling of computers microchips, and heat exchangers. Recently, a new class of heat transfer fluids, called nanofluids, has been developed by suspending

[*] Corresponding author: Yacine Khelili, *khliliyacine1@gmail.com*

nanocrystalline particles in fluids. Nanofluids are thought to be the next-generation of heat transfer fluids. They offer exciting possibilities due to their enhanced heat transfer performance compared to ordinary fluids.

Nanofluids with metallic nano-particles and oxide nano-particles have been investigated by several researchers. A recent development shows that nano-particles can be dispersed in conventional heat transfer fluids such as water, glycol, or oil to produce a new class of high efficiency heat exchange media. *Wang et al*. [1] reported enhanced thermal conductivity for alumina and cupric oxide. Concerning alumina particles, they observed a 12% maximum increase in the conductivity with a 3% volume fraction, while the viscosity showed an increase of 20-30% for the same volume fraction.

Srinivas et al. [2] studied numerically the effect of convection from an isothermally heated circular cylinder for a wide range of power indexes ($0.2 \leq n \leq 1.8$), Reynolds numbers ($1 \leq Re \leq 40$) and Prandtl numbers ($1 \leq Pr \leq 100$). They found that average Nusselt number shows an opposite dependence on power-law index but a positive dependence on Re and Ri numbers.

Dalkilicet al. [3] has reported critical information on theoretical, experimental and numerical work related to forced convection heat transfer of nanofluids. *Anagnostopoulos and Iliadis* [4] used the finite element technique for the solution of steady and unsteady flow around a circular cylinder at $Re = 10^6$ for different blockage ratios. A buoyancy driven mixed convection of nano-fluid around a circular cylinder was presented by *Sarkar et al.* [5]. They showed that presence of nano-fluid minimizes the effect of buoyancy force and stabilizes the flow regime. *Sarkar et al.* [6] investigated numerically mixed convective heat transfer for non-Newtonian nano-fluids around a square cylinder in a vertical flow configuration. They presented the effects of Re, Ri and ϕ numbers (where m and n are values of shear-thinning power-law nano-fluids) on heat transfer. The momentum and forced convection heat transfer for a laminar and steady free stream flow of nanofluids past an isolated square cylinder have been studied numerically by *Farooji et al.* [8]. *Rajaniet al.* [9] investigated a numerical simulation of two and three-dimensional flow past a circular cylinder in different laminar flow regimes. The computation results are validated by measurement data for mean surface pressure, skin friction coefficients, the size and strength of the recirculating wake for the steady flow regime and also for the Strouhal frequency of vortex shedding and the mean and RMS amplitude of the fluctuating aerodynamic coefficients for the unsteady periodic flow regime. The complex three dimensional flow structure of the cylinder wake is also reasonably captured by the present prediction procedure.

Another numerical study on fluid flow and heat transfer around a solid circular cylinder utilizing nanofluid was done by *Valipour and ZareGhadi* [10]. Their results showed that as the solid volume fraction increases, the magnitude of minimum velocity in the wake region and recirculation length increase while separation angle decreases. *Valipouret al.* [11] investigated a numerical simulation to study the fluid flow and heat transfer around a square cylinder utilizing Al_2O_3-H_2O nanofluid for low Reynolds numbers. The Reynolds number varied within the range of 1 to 40 while the volume fraction of nano particles (φ) varied within the range of $0 < \varphi < 0.05$.

Comparison of the single and two-phase modeling for the nanofluids has been considered by the researchers. For instance, *Fard et al.* [12] compared the results of the single phase and two-phase numerical methods for nanofluids in a circular tube. They

reported that for Cu-water the average relative error between experimental data and CFD results based on single-phase model was 16% while for two-phase model was 8%. In another numerical study, *Göktepe et al.* [13] compared these two models for nanofluid convection at the entrance of a uniformly heated tube. Theyfound the same results and confirm the accuracy of two-phase modeling. *Mohyud-Din et al.* [14] in an analytical study, considered the three-dimensional heat and mass transfer with magnetic effects for the flow of a nanofluid between two parallel plates in a rotating system. Three dimensional flow of nanofluids under the radiation (due to solar or etc.) has been analyzed by *Hayat et al.* [15] and *Khan et al.* [16]. They examined the effects of different parameters on the velocity, temperature, skin friction coefficient and Nusselt number of nanofluid flow. Other works of nanofluids flow and heat transfer analysis can be found in literature [17–21].

The present investigation had been motivated by increased interest and research in potential improvements in heat transfer characteristics using nanofluids, typically for flow characterized by low Reynolds number. Effort has been made to study effect of nano-particles on the transport phenomena around a circular cylinder maintained at constant temperature. The problem has been investigated numerically by solving steady state mass, momentum and energy equations. Heat transfer characteristics around the cylinder has been studied for flow having Reynolds numbers less than 40, and using different volume fraction copper nano-particles suspended in water.

Problem Statement and Mathematical Formulation

The present work investigates a two-dimensional problem of a circular cylinder immersed in an incoming flow. The cylinder has a diameter D and its surface is maintained at a constant temperature T_w which is higher than the temperature of the incoming free stream flow, T_∞.

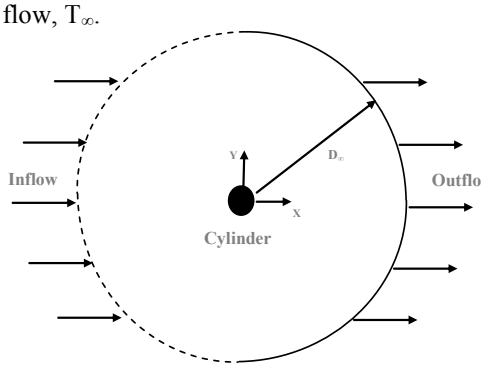

Fig. 1. Schematics of the unconfined flow around a circular cylinder.

This ensures a unidirectional heat transfer from the cylinder surface into the flow stream. The flow far from the cylinder and at the inlet is assumed uniform with free stream velocity U_∞. Numerical simulations are performed for six different nano-particle volume fractions φ. Reynolds number is calculated by using the diameter of the cylinder as a characteristic length.

The minimum value of Re number started from 10, and in order to keep the flow physics essentially in the steady two-dimensional regime, maximum Reynolds number in this study was restricted to 40.

Figure 1 shows the computational domain used in this investigation. The corresponding distance between the top and bottom boundaries is 40D.

At the inlet, a uniform flow was prescribed (U =1, V =0, T_∞ = 0). At the outlet, a homogeneous Neumann boundary condition for the velocity components (U and V) and temperature (T) was used. No-slip conditions were prescribed on the cylinder. At the cylinder surface, uniform temperature (T = 1) was prescribed.

Governing equations

The governing partial differential equations that are Navier-Stokes and energy equations in dimensionless form for two-dimensional incompressible flow (with constant thermo-physical property) are given by equations (1) to (4).

The Reynolds and Prandtl numbers are defined as $Re = \rho U_\infty D/\mu$ and $Pr = \mu C_p/k$.

Continuity Equation:

$$\frac{1}{r}\frac{\partial(rU_r)}{\partial r}+\frac{1}{r}\frac{\partial U_\theta}{\partial \theta}=0 \qquad 1$$

θ-Momentum Equation:

$$\frac{U_\theta}{r}\frac{\partial U_\theta}{\partial \theta}+U_r\frac{\partial U_\theta}{\partial r}+\frac{U_rU_\theta}{r}=-\frac{\rho_f}{\rho_{nf}}\frac{1}{r}\frac{\partial P}{\partial \theta}+\frac{\mu_{nf}}{v_f\rho_{nf}}\frac{1}{Re}\left(\frac{1}{r}\frac{\partial}{\partial r}\left(\frac{\partial U_\theta}{\partial r}\right)+\frac{1}{r^2}\frac{\partial^2U_\theta}{\partial \theta^2}+\frac{2}{r^2}\frac{\partial U_r}{\partial \theta}-\frac{U_\theta}{r^2}\right) \qquad 2$$

r-Momentum Equation:

$$\frac{U_\theta}{r}\frac{\partial U_r}{\partial \theta}+U_r\frac{\partial U_r}{\partial r}-\frac{U_\theta^2}{r}=-\frac{\rho_f}{\rho_{nf}}\frac{\partial P}{\partial r}+\frac{\mu_{nf}}{v_f\rho_{nf}}\frac{1}{Re}\left(\frac{1}{r}\frac{\partial}{\partial r}\left(\frac{\partial U_r}{\partial r}\right)+\frac{1}{r^2}\frac{\partial^2U_r}{\partial \theta^2}-\frac{2}{r^2}\frac{\partial U_\theta}{\partial \theta}-\frac{U_r}{r^2}\right) \qquad 3$$

Energy Equation:

$$\frac{U_\theta}{r}\frac{\partial T}{\partial \theta}+U_r\frac{\partial T}{\partial r}=\frac{k_{nf}}{k_f}\frac{(\rho C_p)_f}{(\rho C_p)_{nf}}\frac{2}{RePr}\times\left(\frac{1}{r}\frac{\partial}{\partial r}\left(\frac{\partial T}{\partial r}\right)+\frac{1}{r^2}\frac{\partial^2T}{\partial^2\theta}-\frac{2}{r^2}\frac{\partial U_\theta}{\partial \theta}-\frac{U_r}{r^2}\right) \qquad 4$$

The fluid properties are described by the density ρ, viscosity μ, thermal diffusivity *a,* and thermal conductivity *k*.

Thermal properties of nanofluids

Density: The density of a nanofluid can be calculated by using mass balance as:

$$\rho_{nf}=(1-\varphi)\rho_{f+}\varphi\rho_p \qquad 5$$

For typical nanofluids with nano-particles of volume fraction less than 1%, a variation of less than 5% in the fluid density is expected.

Specific heat: The specific heat of a nanofluid can be calculated by using energy balance as:

$$(\rho C_p)_{nf}=(1-\varphi)(\rho C_p)_f+\varphi(\rho C_p)_p \qquad 6$$

Where, φ is the nano-particle volume fraction and is given as:

$$\varphi = \frac{Volume\,of\ nano-particles}{Total\,volume\,of\ solution}$$

The Eqs. (5) and (6) were introduced by *Buongiorno* (2006) [28].

Thermal conductivity, by Hamilton and Crosser (1962):

$$\frac{k_{nf}}{k_f} = \frac{k_p + (n-1)k_f - (n-1)(k_f - k_p)\varphi}{k_p + (n-1)k_f + (k_f - k_p)\varphi} \qquad 8$$

where, n = 3 is the shape factor for spherical particles.

Viscosity:

Drew and Passman [29] introduced the well-known Einstein's formula for evaluating for effective viscosity:

$$\mu_{nf} = \frac{\mu_f}{(1-\varphi)^{2.5}} \qquad 9$$

Results and Discussion

The governing equations with the relevant boundary conditions mentioned in previous subsection, were solved by the finite volume method and discretized by QUICK (Quadratic Upwind Interpolation for Convective Kinematics) scheme in space. SIMPLE algorithm was adopted for pressure-velocity coupling calculations. The converged solution of the steady-state problem is obtained when the residual of continuity, X and Y momentum equations, and energy equation is less than 10^{-5}. The thermos-physical properties of the fluid and the nanoparticle, copper, are listed in Table 1.

Table 1. Thermo-physical properties of nano particle and base fluid

	k ($W \cdot m^{-1} \cdot K^{-1}$)	**ρ** ($Kg \cdot m^{-3}$)	**μ 10^{-3}** ($Kg \cdot m^{-1} \cdot s^{-1}$)	**Cp** ($J \cdot kg^{-1} \cdot K^{-1}$)
Water	0.613	997.1	1.003	4179
Cu	400	8933.0	-	385.0

Validation of Results

The solution has been validated by comparing in Table 2, drag coefficient, angle of separation and length of reattachment for Re = 40, which is the largest value in the range considered for simulation. Values obtained in current simulation are found to match closely with data published in literature.

The wake length of the recirculating bubble L_w measured from the rear stagnation point and the separation angle α_s measured from the front stagnation point are shown in Fig. 2.

Table 2. Validation of present work results with literature values for Re = 40

	Authors	C_D	α_s	L_w/D	a/D	b/D
Exp.	*Coutanceau and Bouard*[7]	--	126.2	2.13	0.73	0.59
Num.	*Gautier et al* [22]	1.49	126.4	2.24	0.71	0.59
	Linnick and Fasel[26]	1.54	126.4	2.28	0.72	0.60
	Fornberg[23]	1.50	124.4	2.24	--	--
	Ding et al. [27]	1.58	127.2	2.35	--	--
	Present work	1.50	126.3	2.25	0.71	0.61

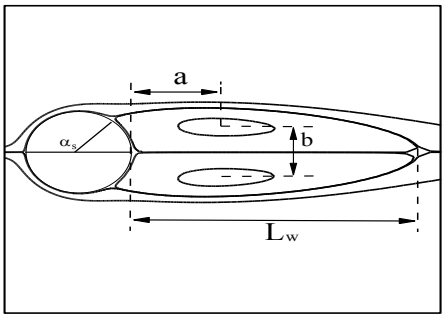

Fig. 2. Wake bubble geometry

Reattachment length

The reattachment length is measured from the downstream side of the cylinder to the point where the velocity changes sign from negative to positive. The comparison between the ratio of the wake length to the cylinder's diameter L/D *vs.* Reynolds number for the solid volume fractions is shown in Figure 3.

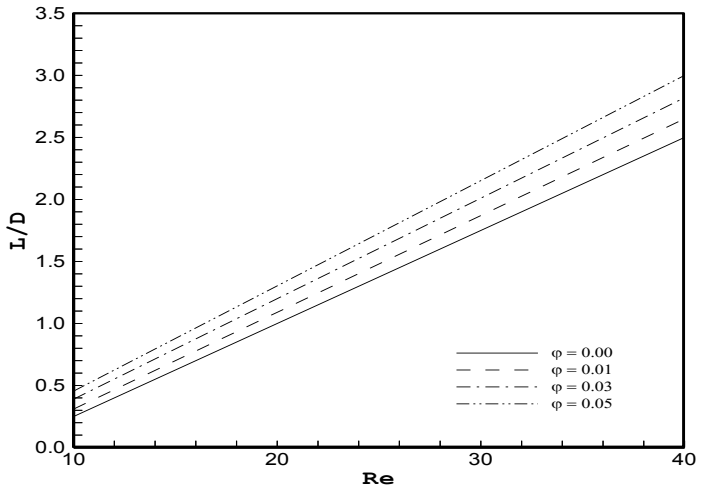

Fig. 3. Variation of wake length with Re at different solid volume fractions φ.

As shown, the wake length increases with increasing Reynolds number. In addition, the wake length increases with increasing solid volume fraction because the flow separation happens earlier in nano-fluid comparing with clear fluid. In nano-fluid, the separation point moves upstream by increasing the solid volume fraction.

Flow separation occurs when the streamlines no longer remain attached to the body and causes wakes near the surface. Angular position of the separation point is a function of Reynolds number. Figure 4 shows the relationship of α_s with respect to Re. It is clear that the point of separation travels upstream with increasing Re.

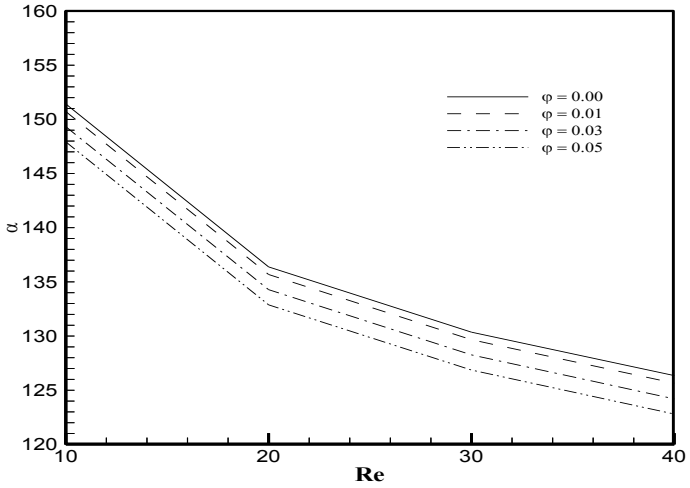

Fig. 4. Variation of separation angle with Re at different solid volume fractions φ.

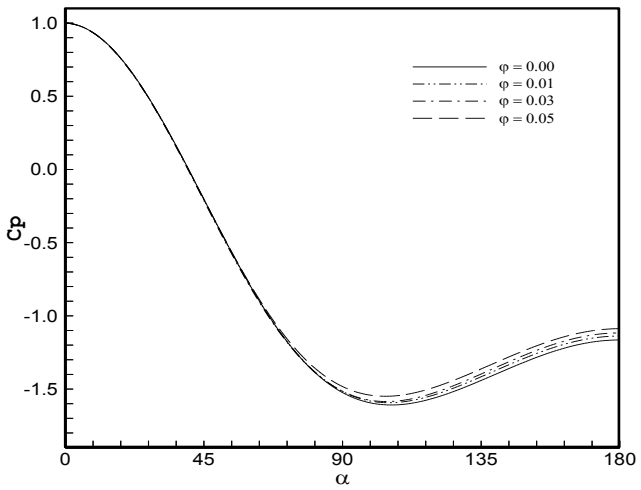

(a)

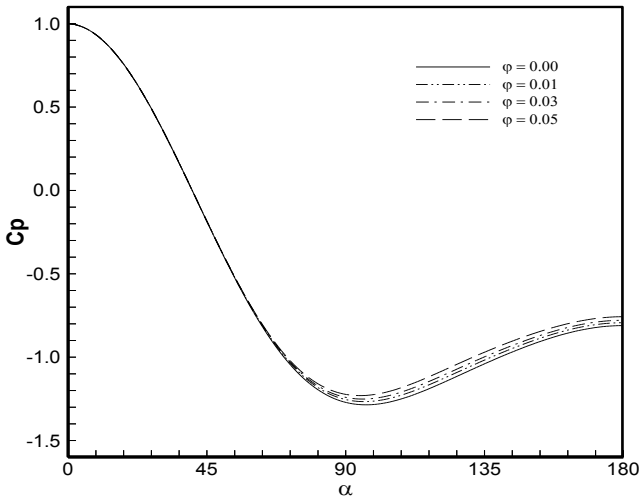
1.0
0.5
0.0
-0.5
-1.0
-1.5
Cp
0
45
90
135
180
α
φ = 0.00
φ = 0.01
φ = 0.03
φ = 0.05

(b)

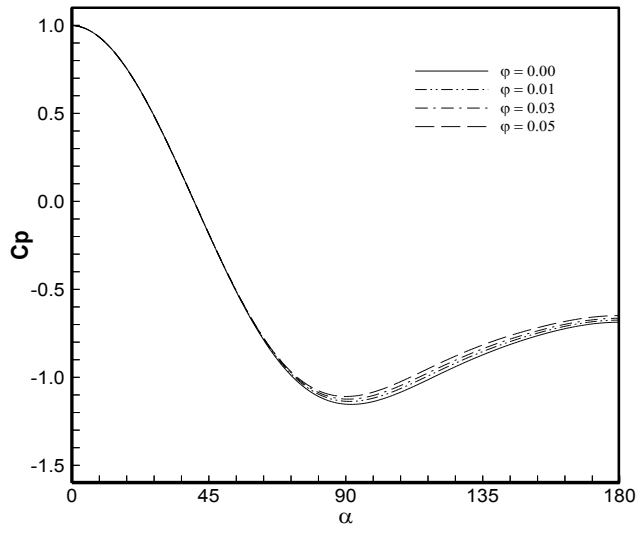
1.0
0.5
0.0
-0.5
-1.0
-1.5
Cp
0
45
90
135
180
α
φ = 0.00
φ = 0.01
φ = 0.03
φ = 0.05

(c)

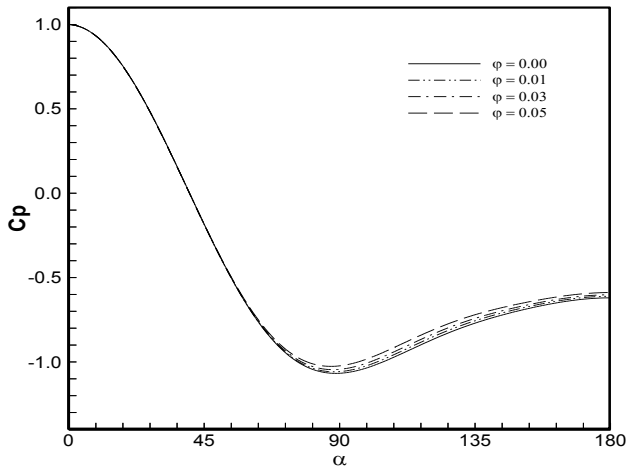

(d)

Fig. 5. Distribution of pressure coefficient around surface of cylinder for various solid volume fractions φ at a) Re = 10, b) Re = 20, c) Re = 30, d) Re = 40.

Effect of nano-particle loading on cylinder forces

The presence of nano-particles in the fluid influences the pressure distributions on the cylinder surface (Fig. 5). The value of pressure coefficient increases in the adverse pressure gradient region because the inertial forces, hydrodynamic boundary layer thickness and the viscosity increase with increasing values of solid volume fraction. The pressure coefficient is defined by:

$$Cp = \frac{P - P_0 + 0.5\rho U_\infty^2}{0.5\rho U_\infty^2} \qquad 10$$

Effect of nano-particle on flow characteristics

The streamlines, vorticity and isotherm contours around cylinder are compared between clear fluid and nanofluid (φ = 0.05) in Figure 6, for Reynolds number of 10, 20, 30 and 40. It can be seen that the re-circulation length increases as Reynolds number increases in both clear and nano-fluid. However, in nano-fluid the center of the wake is slightly shifted away from the surface of the cylinder comparing with clear fluid. The strength of the vorticity is increased in comparison with the nano-fluid. For the temperature distribution contours, it can be concluded that the temperature contours are steeper in the near-wake region with increasing Reynolds number. This means that a higher Reynolds number sets a higher temperature gradient. It can also be seen that the nanofluid shows a higher heat transfer rate from the cylinder than the clear fluid.

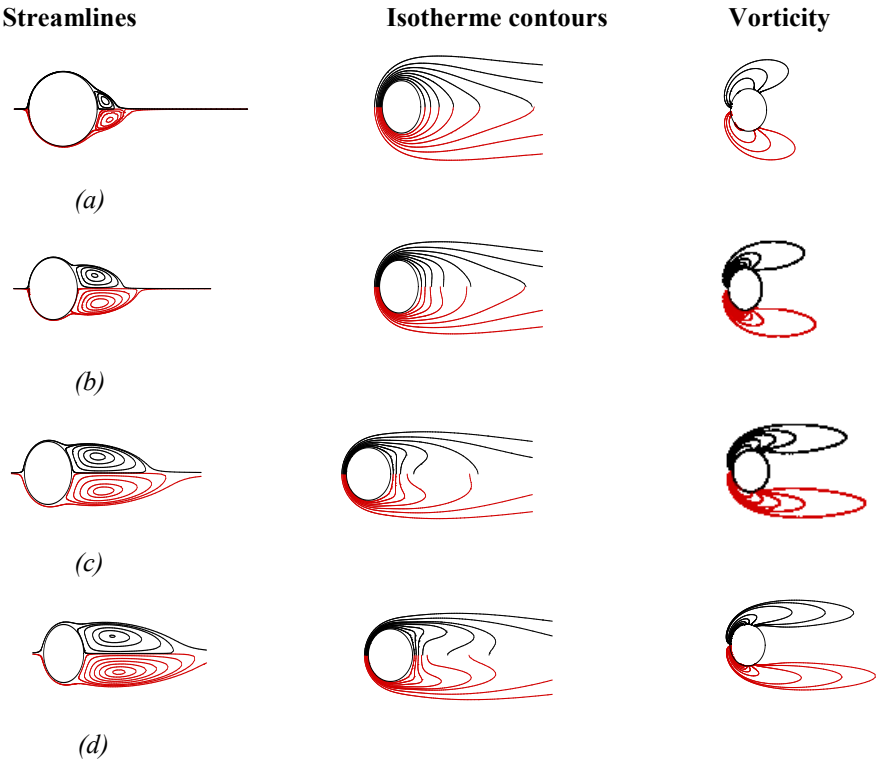

Fig. 6. Streamlines, vorticity and isotherm contours around the cylinder, ((clear fluid (black lines) and water/Cu 5% (red lines)) at: a) Re = 10, b) Re = 20, c) Re = 30, d) Re = 40.

Effect of nano-particle on augmentation in heat transfer

In this section, we investigated the effect of nano-particle volume fraction on heat transfer performance of nanofluid. The quantification of heat transfer is characterized by local and average Nusselt number. For a nano-fluid, the Nusselt number is a function of various factors such as heat capacitance and thermal conductivity of both the base fluid and the nano particles, the volume fraction of suspended particles, the viscosity of the nanofluid as well as the wake structure.

The local Nusselt number of the nanofluid, based on cylinder diameter is defined as:

$$\mathrm{Nu} = -\left[\frac{k_{nf}}{k_f}\frac{\partial\theta}{\partial n}\right]_{\text{along the cylinder surface}} \qquad 11$$

Surface averaged Nusselt number of fully developed thermal boundary layer is defined as:

$$\mathrm{Nu}_{\mathrm{ave}} = \frac{1}{s}\int_{s} \mathrm{Nuds} \qquad 12$$

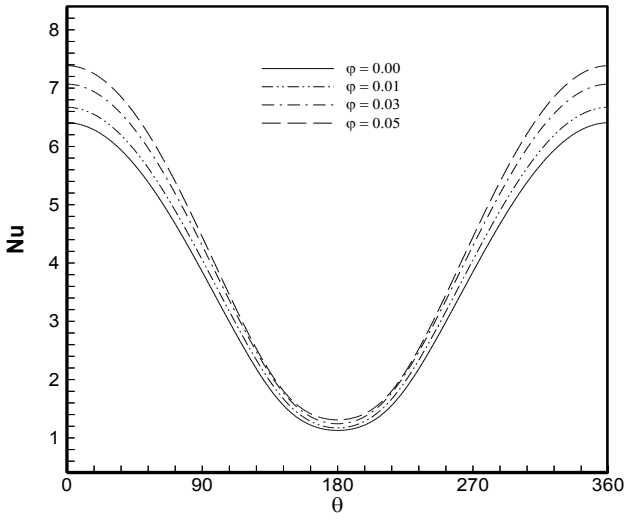

(a)

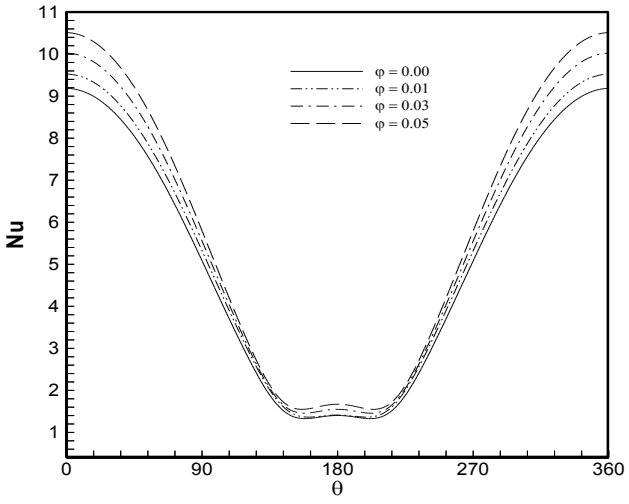

(b)

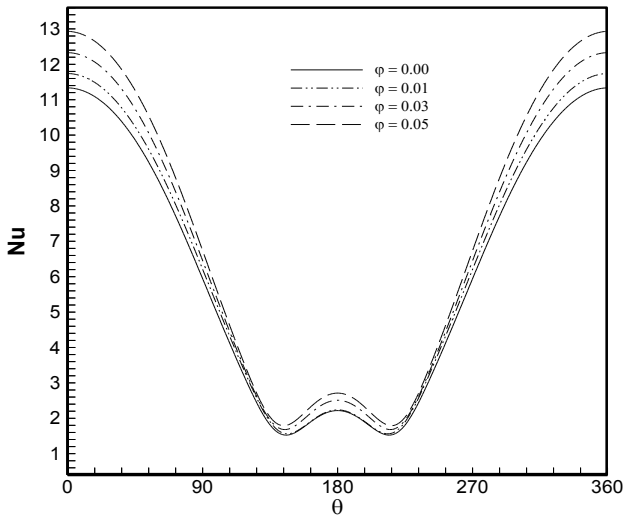

(c)

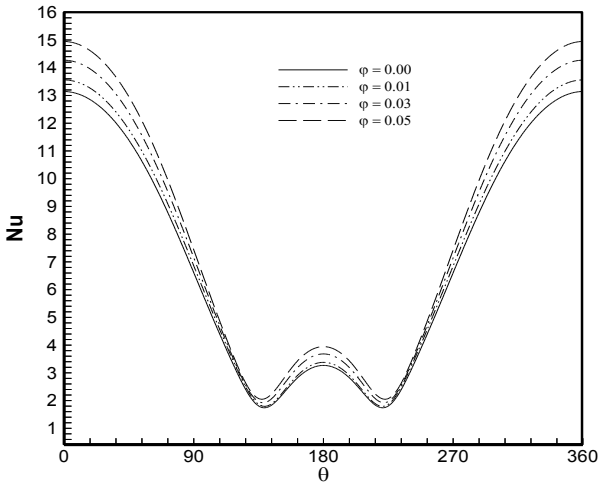

(d)

Fig. 7. Variation of local Nusselt number on cylinder surface with various solid volume fraction φ at a) Re = 10, b) Re = 20, c) Re = 30, d) Re = 40.

A comparison between local Nusselt numbers along the cylinder for various solid volume fractions and Reynolds number was shown in Figure 7. It can be seen that Nusselt number increases with increases in solid fraction and in Reynolds number. However, the reason for increase in the two cases is entirely different.

Variation of average Nusselt number for different values of Reynolds number and solid fraction is shown in Figure 8 and Figure 9, respectively. In these figures it is shown that increasing both Reynolds number and solid volume fraction will increase the average Nusselt number. One of the main reasons for this behavior is:

- the motion of nano-particles that transport heat energy.
- the micro-convection of fluid surrounding nano-particles.

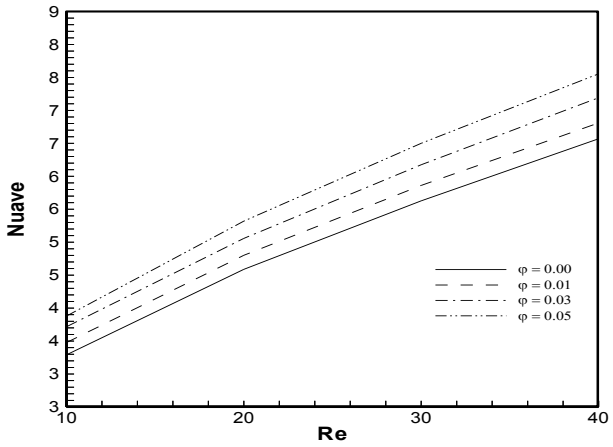

Fig 8. Variation of average Nusselt number on the wall of cylinder versus Reynolds number for different solid volume fractions, φ.

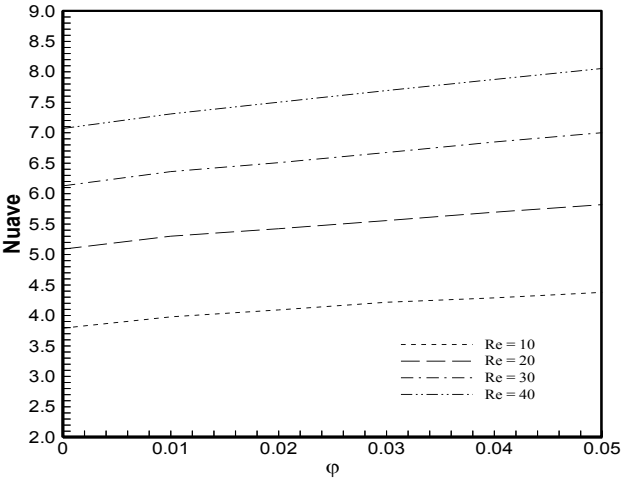

Fig 9. Variation of average Nusselt number on the wall of cylinder versus solid volume fractions, φ for different Reynolds number.

Conclusion

Steady laminar flow behind a circular cylinder, has been subjected to numerous experimental and computational studies. One of the most prominent flow structure change takes place in the vicinity of Re < 40. Below this Reynolds number, the flow is characterized by the presence of a symmetric pair of closed separation bubbles. Beyond Re = 40, the flow becomes unsteady and asymmetric, and alternate vortex shedding begins. In this article, the point of investigation was to evaluate the effect of nano-particle on convective heat transfer and flow characteristics. It is observed that the vorticity, pressure coefficient, recirculation length is increased by the addition of nano particles into clear fluid. Moreover, the local and mean Nusselt numbers are enhanced due to adding nano-particles into base fluid.

Nomenclature

C_D	coefficient of drag, [–]
D	cylinder diameter, [m]
k	thermal conductivity, [Wm^{-1} K^{-1}]
P	non-dimensional pressure, [–]
Pr	Prandtl number, $(= \nu/a)$, [–]
Re	Reynolds number, $(= \rho U_\infty D/\mu)$, [–]
T	non-dimensional temperature
U_r, U_θ	non-dimensional velocity components, [–]
r, θ	non-dimensional coordinates, [–]
Greek symbols	
μ	dynamic viscosity, [kg $m^{-1}s^{-1}$]
ρ	density, [kg m^{-3}]
ν	kinematic viscosity, [m^{-2} s^{-1}]
α	separation angle [°]
Subscripts	
∞	free stream
w	wall
ave	average
f	fluid
p	solid
nf	nanofluid
s	separation of flow
0	stagnation point

References

[1] X. Wang, X.Xu, S.U.S Choi:J Thermophys Heat Transfer, 13 (1999) 474-480.
[2] A.T. Srinivas, R.P. Bharti, R.P.Chhabra:IndEngChem Res, 48 (2009) 9735-9754.
[3] A.S. Dalkilic, N. Kayaci, A. Celen, M. Tabatabaei, O. Yildiz, W.Daungthongsuk, S. Wongwises:CurrNanosci, 8(2012) 949-969.
[4] P.Anagnostopoulos, G.Iliadis: Int J Numer Methods Fluids, 22 (1996) 1061-1074.
[5] S. Sarkar, S. Ganguly,G. Biswas:Int J Heat Mass Transfer, 55 (2012) 4783–4799.
[6] S. Sarkar, S. Ganguly, A. Dalal:Int J Heat Mass Transfer,59(2013) 433-450.
[7] M.Coutanceau, R.Bouard:J Fluid Mech79 (1977) 231–56.
[8] V. Etminan-Farooji, E.Ebrahimnia-Bajestan, H. Niazmand, S. Wongwises: Int J Heat Mass Transf 55 (2012) 1475–1485.
[9] B.N. Rajani, A. Kandasamy, S. Majumdar:App Math Mod, 33 (2009) 1228–1247.
[10] M.S. Valipour, A.Z. Ghadi: Int Communication in Heat and Mass Transfer, 38 (2011) 1296-1304.

[11] M.S. Valipour, R.Masoodi, S. Rashidi, M. Bovand, M. Mirhosseini:ThermSci, 18 (2014) 1305-1314.
[12] M.H. Fard, M.N. Esfahany, M.R. Talaie:IntCommun Heat Mass Transfer, 37 (2010) 91–97.
[13] S.Göktepe, K. Atalik, H. Ertürk:Int J ThermSci, 80 (2014) 83–92.
[14] S.T. Mohyud-Din, Z.A. Zaidi, U. Khan, N. Ahmed: AerospSciTechnol46 (2015) 514-522.
[15] T. Hayat, M.Imtiaz, A.Alsaedi, M.A. Kutbi:J Magnet Magnet Mater 396 (2015) 31–37.
[16] J.A. Khan, M. Mustafa, T. Hayat, A. Alsaedi: Int J Heat Mass Trans, 86 (2015) 158–164.
[17] M. Hatami, D.D. Ganji: Thermal Eng, 2 (2014) 14–22.
[18] M. Fakour, A. Vahabzadeh, D.D. Ganji, M. Hatami: JMolLiq 204 (2015) 198–204.
[19] S.E. Ghasemi, M. Hatami, A.K. Sarokolaie, D.D. Ganji:Phys E: Low-DimenSystNanostruct, 70 (2015) 146–156.
[20] S.E. Ghasemi, M. Hatami, GH.R. MehdizadehAhangar, D.D. Ganji: JElectrostat 72 (1) (2014) 47–52.
[21] G. Domairry, M. Hatami: J MolLiq, 193 (2014) 37–44.
[22] R. Gautier, D. Biau, E. Lamballais: Comput Fluids, 75 (2013) 103–111.
[23] B. Fornberg: J Fluid Mech, 98 (1980) 819–55.
[24] K.V.Wong, O. De Leon:AdvMechEng (2010) ID 519659, doi:10.1155/2010/519659.
[25] R. Taylor, S.Coulombe, T.Otanicar, P. Phelan, A.Gunawan, W.Lv, G. Rosengarten, R.Prasher, H.Tyagi: J ApplPhys, 113 (2013) doi: 10.1063/1.4754271.
[26] M.N.Linnick, H. Fasel:J ComputPhys,204 (2005) 157–92.
[27] H.Ding, C.Shu, Q. Cai:Comput Fluids, 36 (2007) 786–93.
[28] Buongiorno J: J Heat Transfer, 128 (2006) 240–250.
[29] D.A. Drew, S.L. Passman, Theory of multicomponent fluids Vol. 135, Springer Science & Business Media, Berlin, 2006.